Characterization of the radio communication channel in forest fire environments

Pedro António Gomes Duarte Coimbra
pedro.d.coimbra@tecnico.ulisboa.pt
Instituto Superior Técnico

***Abstract*—Wildfires are a recurring phenomenon in many countries around the world, either due to natural causes or negligent use of agricultural machines. Emergency communication services used by firefighters at the theatre of operations must be highly reliable, in order to ensure the safety and coordination of the teams that are fighting the wildfire, thus extinguishing it as quickly as possible with minimum use of resources. Emergency communication networks strongly rely on wireless links that may be obstructed by the flames. However, little attention has been given to studying the propagation of radio waves in extreme fire environments. In this thesis, we propose the embryo of a simulation tool, that is intended to predict within affordable computation time the outage of a communication. To overtake this goal, it is necessary to study and quantify the attenuation caused by wildfires on the electromagnetic waves propagation path. This is a relevant and current research topic, given the unpredictable behaviour of wildfires, which may jeopardize civil protection forces, thus emphasizing the need for preventing the outage of emergency services even for a few minutes. Furthermore, the properties of the medium require a higher preparation. Numerical results showed an RF attenuation of 3 to 7 dB for a maximum number of four trees. Experimental results showed that the impact on the link is larger when vegetation is burned. The embryo of the new simulation tool computational performance gives good prospects for the future. However, to reach its full purpose needs to be fed with larger numerical and experimental validation. For the future of the project it is necessary to test and measure the attenuation for larger volumes of vegetation and adapt the simulation tool to the new data.**

***Index Terms*—Broadband antenna, communication outage, propagation of electromagnetic waves, plasma frequency, radio frequency attenuation.**

I. Introduction

Wildfires are a recurrent problem affecting many areas of the world and year after year an enormous amount of resources are allocated to fight this phenomena. Only during the last decade it was possible to testify gigantic tragedies related with wildfires. In 2017, Portugal was afflicted by the deadliest wildfires in the country's history where dozens of people were killed and hundreds were injured. Likewise, in 2020 Australia struggled to overcome the fires that swept and damaged its population and unique wild life. Due to these events, there is a world and specially national effort to understand and study the key processes to avoid future tragedies. Among these processes is the propagation of electromagnetic waves under fire conditions.

Radio communications systems play a major role in the fighting process as they allow fire fighters to coordinate and cooperate their efforts to control bushfire outbreaks. Since the introduction of radio communications to emergency services, the topic of propagation of radio waves in extreme fire environments has not been addressed with the deserved attention even though there is evidence that radio communications can be degraded when close to the fire. [1] Under fire conditions, electromagnetic waves propagation paths have to cross extensive fire fronts and so it is pertinent to study and quantify the effects caused by the fire. The main effects are refraction, dispersion and absorption of the electromagnetic waves which results in an attenuation of the signal. This problem is specially relevant when affecting public safety and emergency services on the move like Terrestrial Trunked Radio (TETRA) networks but also in the common mobile networks like GSM, 3G and 4G. However, when addressing this topic it is necessary to have a model that describes the physical phenomena that is attenuation.

The unpredictability of a wildfire allied with its dependence on the ground characteristics, surrounding atmosphere and vegetation characteristics make the goal of achieving an analytical model not easily reachable. Thus, the main challenge is to build a bridge between two different fields: thermodynamics and electromagnetism. Thermodynamics gives the combustion characterization whereas the electromagnetism uses this acquired knowledge to predict the signal attenuation. The existing thermodynamics and electromagnetic simulation tools have long running times, even just for small-size scenarios (e.g.single tree), which makes impossible to compute real time data about the signal attenuation when facing an enormous wildfire. Therefore this thesis proposes as a final goal the embryo of a simulation tool, that is intended to predict within affordable computation time the outage of the communication between a certain base station and the users near the fire front. This simulation tool is intended to be used during a forest fire to evaluate and predict the risk of communication failures in order to avoid them. This real time data and prediction can be key to adapt the communications among the people involved to the real time fire characteristics. To achieve this goal several steps are required: characterizing the propagation of electromagnetic waves in wildfire conditions, simulation and studies of different flora species to build a database, measurement campaigns under controlled fire conditions to compare and validate the existing simulations tools. Using the built database, and user defined input parameters like terrain characteristics, dominant type of trees, density of the forest and some parameters related with the atmosphere conditions it should be possible to reach a faithful prediction of the signal

attenuation within affordable computation time.

II. State of the Art

Flames have puzzled the research community for a long time, with special interest in its electrical characteristics. Since the 19th century, when G. Erman obtained currents from flames by inserting two wires in them, it has been known that flames possess a high electrical conductivity and can be distorted by an electric field [2]. Early studies address the topic of radio propagation in fire environments in detail and prove that flames have indeed conductive properties, where charged particles are generated as a product of combustion [1], [3], [4]. Furthermore, [5]–[7] measurements acknowledge that some frequency bands, particularly VHF (Very High Frequency) and UHF (Ultra High Frequency) communication bands, are affected by fire, being attenuated when fire is present. Ionization, present in the flames, is identified as the major cause of attenuation on radio propagation.

The vegetation that is normally involved in the combustion process during a forest fire is mostly made up of cellulose, hemicellulose, lignin, extractives and mineral mater such as alkali-alkali metals [6]. When these components are exposed to fire extreme temperatures, thermal-ionisation occurs thus generating an ionised plasma [6]. A plasma is a state of matter that contains charged particles that move freely [1]. The interaction between these free electrons and the electromagnetic waves results in dispersion and attenuation. Small scale fire experiments performed by Boan in [1] have demonstrated that attenuation of radio energy occurs in the presence of fire and that it is dependent on the frequency band and also if fire intercepts the line of sight propagation path. In addition it is stated that this attenuation also correlates to fire's intensity and size, meaning that combustion of plant life can be enough to cause communication problems. During a forest fire, the attenuation caused by the ionised plasma is enough to result in degradation of signal strength and link quality as shown in [8].

This ionised plasma problem is not only addressed in the forest fires context. Rocket plume literature is also quite useful as it struggles with the same two problems: the specification of the plasma parameters and the calculation of the effect of the plasma on the electromagnetic waves which have to overcome the attenuation caused by the plasma at re-entry in the atmosphere. The high quality reception of radio waves it is also very important to guarantee security during the flight. Unfortunately, the propagation of emitted and received waves is disturbed by the exhaust plume of the launcher [9]. Recent studies such as [10], [11] propose more reliable numerical models of electromagnetic interaction based on Finite Difference Time Domain method (FDTD). FDTD formulation is a convenient tool for solution of electromagnetic wave problems. Considered to be a scattering algorithm it utilises finite difference approximations to calculate the space and time derivatives of Maxwell's equations [1]. Since its introduction, FDTD has been used in studying electromagnetic (EM) wave propagation through dispersive mediums where the permittivity and/or permeability are functions of the frequency [12]. When used to analyse and study simple shapes of the plasma, the FDTD method gives satisfactory results. Unfortunately the reality is that rocket plumes, just like forest fire plumes, are of arbitrary shape and the use of a staircase mesh in FDTD method may lead to significant errors [9]. [13] underlines this strict geometry limitations. FDTD requires time consuming numerical calculations, especially in complex geometries and large volumes.

In order to compute the RF attenuation associated with a communication that has its propagation path through a forest fire it is necessary to know the electrical proprieties of the plasma such as the electron density and electron collision frequency. The electrical properties of the ionized plasma are dependent on the temperatures reached during the combustion process and on the chemical characteristics of the released gases. The Fire Dynamics Simulator (FDS) [**?**] emerges as an alternative to compute these combustion related parameters.FDS is a three dimensional thermodynamic solver, which includes combustion modelling. FDS is adequate to build a spatial and temporal picture of the fire and the gases involved for building a propagation model [1]. Studies like [14] show that FDS model predictions of mass loss rate and radiative heat flux compare reasonably well to measurements. Despite being a robust and accurate tool, FDS has also some important handicaps. [15] highlights that FDS simulations are time consuming and computationally heavy. Although these issues can be minimized with the use of powerful computers, with the long running times of FDS simulations it is not possible to make real time analysis of a certain plasma characteristics when a forest fire starts.

III. Background theory

A. Propagation

The main focus of this work is the influence of fire on the propagation path, independent to the background. When burning vegetation, it is known that leaves, trunk and branches cause attenuation to the electromagnetic waves. This work focuses only on the excess attenuation that is caused by the fire itself.

1) Refraction in Fire Environments: Refraction of an electromagnetic wave is the phenomenon of change of propagation direction when it goes from one medium to another. The most common reason for refraction to happen is change in the velocity of propagation due to change in medium [16]. Whenever electromagnetic waves propagates through a fire front, it experiences the effect of a medium that is randomly and constantly changing. In ordinary atmospheric circumstances, radio waves curve lightly toward the earth surface because the pressure and temperature profile cause a higher refractive index at ground level [8]. However, the temperature increment and presence of electrons in the flame lowers its refractive index, thereby creating a medium of spatially varying refractive index. Therefore, incident radio waves change speed and are consequently deflected from their original path. This refraction has an effect of decreasing signal

intensity at a targeted receiver [17]. The refractive index is related to the relative permittivity of the medium as:

$$n_r = \sqrt{\epsilon_r} \tag{1}$$

The plasma is characterized by a frequency dependent permittivity given by the Drude relation:

$$\epsilon_r(\omega) = 1 - \frac{\omega_p^2}{\omega(\omega - iv_e)} \tag{2}$$

where v_e is the electron collision frequency (s^{-1}), ω_p the plasma frequency (s^{-1}) and ω the frequency ($\omega = 2\pi f$). The plasma frequency describes the frequency at which the electron density varies in the plasma:

$$\omega_p = \sqrt{\frac{N_e q_e^2}{\epsilon_0 m_e}} \tag{3}$$

where N_e is the electron density (m^{-3}), q_e is the electron charge ($1.602\times10^{-19}A\cdot s$), m_e is mass of an electron ($9.109\times 10^{-31}Kg$), and ϵ_0 is permittivity of vacuum ($(36\pi\times10^9)^{-1}s^4\cdot A^2\cdot Kg^{-1}\cdot m^{-3}$) [9].

2) Diffraction in Fire Environments: Diffraction occurs when the electromagnetic waves pass through small openings, around obstacles or by sharp edges [18]. This phenomenon is only possible due to the elastic properties of electromagnetic waves. Whenever an electromagnetic wave is blocked due to an obstacle there is a formation of a shadow region, with radio energy, behind this same obstacle. There is a relation between diffraction and the wavelength (λ): longer wavelengths exhibit greater diffractive recovery in the shadow region [1]. Diffraction is a meaningful phenomenon in the context of forest fires because when the propagation path is obstructed by a fire or a tree, this radio energy may still propagate into the shadow region.

3) Scattering in Fire Environments: As scattering is caused by sudden changes in the propagation medium, this phenomena is also important in the context of forest fires. The medium during a forest fire is in constant and unpredictable change. These changes cause radio energy to be scattered in different directions. Scatter occurs in the fire environment specially in two different ways: due to the airborne debris or particles swept up by the convection currents of the combustion region and caused by air movements in the atmosphere surrounding the fire [1].

B. Fire Background Physics

1) Chemi-Ionisation: Chemi-Ionisation is a process in which ionised particles are created in hydrocarbon chemical reactions. As referred, forest fires have mostly flora as its main fuel. This flora vegetation usually involved in the combustion process is mainly composed for lignin ($C_{40}H_{40}O_6$) and cellulose ($C_6H_{10}O_5$) which are both large hydrocarbon molecules. During the combustion, the process of chemi-ionization tends to break these large molecules into simpler particles like electrons that usually concentrate in the reaction zone of the flame. [1] [19]

2) Thermal-Ionisation: The combustion fuel of a forest fire, plant life, generates an extremely hot environment where temperatures can reach values higher than 1200K. This high temperature environment thermally excites incumbent flame particles. The energized particles become electronically unstable, to the extent that they lose their outer shell electrons on collision with other flame particles, a process that occurs on selective basis determined by temperature and ionization potential. This process is called thermal ionization [20]. During a forest fire, the species that are present in plant life and could undergo thermal ionisation are alkali and alkaline earth metal such as potassium and calcium, and graphitic carbon [17]. Prior to combustion, there are two important processes that increase the chances of occurrence and spread of forest fires: drying and pyrolysis. The drying process doesn't need hot temperatures to occur, a simple very hot summer can take care of it. After the drying process it occurs pyrolysis. This process is the delivery of solid fuel into a gaseous state that then enters the combustion zone [1]. Basically the dramatic sequence of processes in forest fires is drying, pyrolysis and finally the combustion.

3) Plasma in Fire Environment: Plasma is a state of matter that results from the processes of chemi-ionisation and thermal-ionization that result in the creation of charged particles. Hence, plasma is composed by charged particles that freely move [1]. Ionized electrons interact with electromagnetic waves, resulting dispersion and attenuation [8]. This resulting attenuation in the signal is specially influenced by three different parameters that characterize the plasma: temperature, electron density and electron collision frequency. The electron collision frequency is the probability of collision between an electron and another species [9]. In this work, the collision frequency is estimated using the following equation:

$$\phi_{eff} = 7.33\times10^3 N_m a^2\sqrt{T} \tag{4}$$

where T is temperature, N_m is number density of air molecules and a is the radius of an air molecule [21]. The electron density is the the number of free electrons due to the ionization processes. For a known fuel volume, using the Fire Dynamics Simulator it is possible to compute the fuel density that is in gas state due to the pyrolysis processes. As referred, the main elements that take action in these processes are Potassium (K), Calcium (Ca) and Magnesium (Mg). Hence, it is possible to calculate the concentration of each element using the following equation:

$$N_X = N_{fuel}\times\rho_X\times\Pi_X \tag{5}$$

where ρ_X is the percent of each element (K, Mg, Ca) present in the part of the plant that is burnt, and Π_X is a pyrolysis coefficient encapsulating the ease of pyrolysis by the element [1]. Lastly, it is possible to calculate the free electron density using the following equations:

$$N_e^- = \sqrt{K_1 N}\left[\sqrt{1+\frac{K_1}{4N}} - \sqrt{\frac{K_1}{4N}}\right] \tag{6}$$

where N encompasses the total number of atoms present being neutral or ionised and K is given by:

$$K_1 = 2\frac{P_M^+}{P_M}\left(\frac{2\pi m_e kT}{h^2}\right) exp\left(-\frac{E_i}{kT}\right) \quad (7)$$

where P is the internal partition fraction, m_e is the electron mass, K is the Boltzmann's constant, h is the Planck's constant, T is the temperature and E_i is the ionisation potential [1].

IV. Transmission Line Method (TLM)

Consider the geometry of figure 1, that shows the geometry of a single-tree scenario. The volume containing and surrounding the tree is split into $m \times n$ longitudinal dielectric tubes as represented in figure 1, assuming wave propagation along the z-axis. Each of these tubes is itself split into voxels, as shown in figure 2, each one with its electrical properties (ϵ, σ) according to the local vegetation filling and fire state.

The Transmission Line Method (TLM) is used recursively calculate the S-parameters of a cascade of transmission lines, along z. The method takes proper account of the multiple incident and reflected waves propagating in the system.

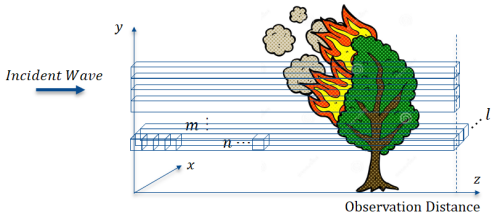

Fig. 1: One tree geometry illustration.

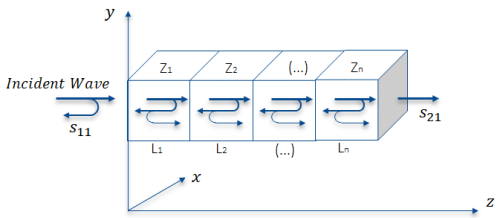

Fig. 2: Multiple reflections illustration.

Among different formulations that can be used to model analytically this problem, this work deals with the ABCD matrix method. The ABCD matrix of the cascade connection of two or more two-port networks is found by successive multiplication of the ABCD matrices of the individual two-ports networks. In a lossy medium, as the one that is present in a fire environment, the ABCD matrix in each slab is given by [22] :

$$\begin{bmatrix} A & B \\ C & D \end{bmatrix} = \begin{bmatrix} cosh(\gamma l) & jZsinh(\gamma l) \\ jYsinh(\gamma l) & cosh(\gamma l) \end{bmatrix} \quad (8)$$

where γ is given for:

$$\gamma = j\omega\sqrt{\mu_0\epsilon_0\epsilon_r} \quad (9)$$

where Z and Y are the impedance and admittance of the slab, l represents the length of the slab, μ_0 and ϵ_0 are the vacuum permeability and permittivity and finally ϵ_r represents the relative permittivity of the unit cell.

The main issue in the beginning was to prove that this method could be used for plasma media. Hence, we numerically calculated the S-matrix of five cascaded slabs with arbitrary relative permittivity values commonly found in plasma media. Figure 3 and 4 show the S parameters results for the 5 slabs case, over a 10 GHz frequency range. In addition, a validation for a 81 slab case can be found in [23]. A good correspondence was found between the TLM method and the full-wave CST results obtained for the same case.

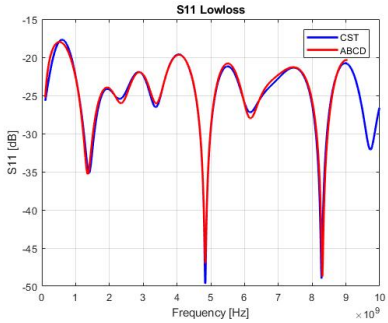

Fig. 3: S11 results for the five slabs simulation.

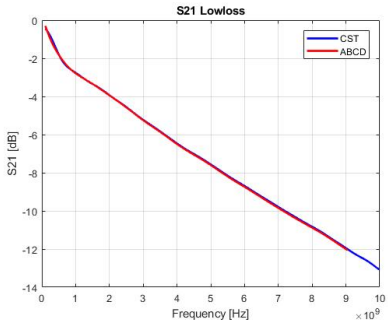

Fig. 4: S21 results for the five slabs simulation.

V. Numerical Results

This section describes the obtained results on the post-analysis for some of the Fire Dynamics Simulator simulations performed during this work. In this section are compared four different small scale simulations for one tree species that is Eucalyptos Diversicolor. All these different small scale simulations were for the frequency of 385 MHz which corresponds to the TETRA frequency in Portugal. For these cases, a plasma with A-AEM quantities of K=0.9%, Ca=0.82% and Mg=0.28% was generated to simulate the combustion of the trees in the different simulations. All the plots and explanations are presented next for the simulation with one tree. Afterwards, a comparison is made with the simulations for two trees in line, four trees in line and four trees in a square.

A. One Tree Simulation Post-Analysis

The full computation volume of $4 \times 4 \times 8$ m was divided in voxels of $5 \times 5 \times 5$ cm. This meaning that the dataset is

divided in 81 slices of 161x81 and forming 161 tubes of 81 voxels each. The scenario was simulated for a duration of about 30 s which corresponds to 1002 time instants of the fire dynamics simulator and 3-dimensional profiles of temperature and gases densities were recorded for post-processing. Figure 5 presents a dataset illustration with the marked axis as well as a slice illustration in the right figure.

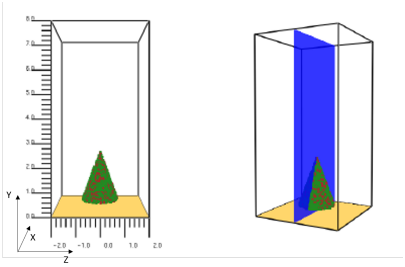

Fig. 5: One tree simulation dataset illustration.

We can analyze the combustion temperature profile evolution from a slice (e.g. represented slice in figure 5). The ignition process starts around the instant 10. The temperatures then continue to increase and the higher temperatures for this dataset are comprehended between the instants 200 and 486. The maximum value for the combustion temperature reached for this dataset is 1461 K. Temperature profile plot for the instant where the maximum temperature is reached can be found in figure 6. After the instant 500, the maximum temperatures start to drop.

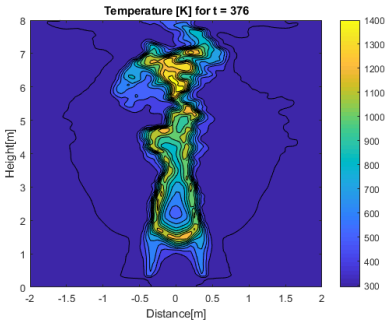

Fig. 6: Temperature profile for the middle slice of the dataset for the instant 376, where the maximum combustion temperature is reached.

The evolution of the temperature is specially important to understand the evolution of the fire and to locate the possible maximums of attenuation. Hence, using the plasma parameters explained before, we can compute the reflection and transmission coefficients along the z direction for the whole volume of the dataset. Figure 7 shows a cumulative distribution function for the S_{11} values for the whole volume of the dataset, for the instants where the combustion is more active. From the cdf it is understandable that the study of the reflection coefficient will not have a big expression to the problem. In the presented dataset the x-axis scale was limited to -100 dB and the probability of finding values below this threshold is still large.

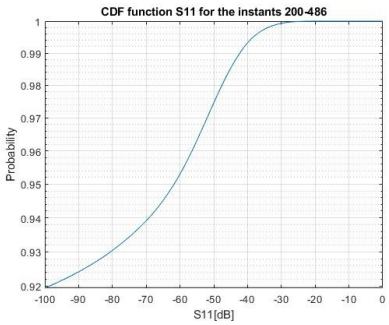

Fig. 7: CDF for the S11 values, for all the tubes, for the time instants where the combustion is more active.

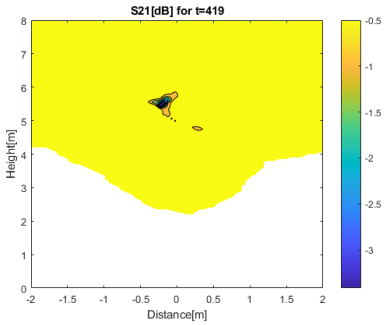

Fig. 8: S21 results for the maximum attenuation time instant.

Figure 8 presents the S_{21} results for the maximum attenuation time instant, for this dataset. The minimum value reached for this metric is -3.42 dB. The transmission coefficients results allow to compute the attenuation in each tube. Two different attenuation computations are done in this work: the attenuation rate α and also the squared absolute value of the transmission coefficient. The reason for this second metric is that it does not depend on the size of the dataset and so it is useful for comparison when the datasets have different dimensions. Starting with this second computation, this indicator presents a maximum value of 3.42 dB whereas maximum value for the attenuation rate α is 0.84 dB/m. Although this values already have some expression it is important to highlight that these values are recorded in one cell. For the whole volume of the tree there are 161×81 tubes and these values are registered only in one cell which may or may not affect the link depending on its location. The low probability of these values it is understandable for the cdf function for the S_{21} values, for all the tubes and time instants where the combustion is more active, presented in figure 9.

B. Comparison with larger datasets

Table 1 shows the attenuation results for four different scenarios: one tree, two trees side by side, four trees side by side and four trees disposed in a square. These four different simulations showed some interesting common characteristics that deserve to be highlighted.

For all the four different scenarios the temperature profiles showed some similarities with the ignition being around instant 10, the instants where the combustion is more active

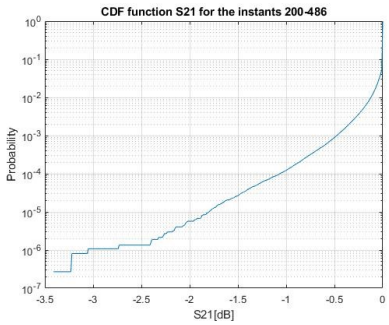

Fig. 9: CDF for the S21 values, for all the tubes, for the time instants where the combustion is more active.

TABLE I: Attenuation maximum values summary

Max Values	1 Tree	2 Trees	4 Trees	4 Trees in Square
$\mid S21 \mid^2 [dB]$	3.42	4.22	6.46	7.24
$\alpha[dB/m]$	0.84	1.04	0.80	1.79

being comprehended between instants 200 and 486 and after instant 500 the maximum temperatures starting to drop. In addition, for all the simulations the maximum of temperature reached was in the order of magnitude of 1400 K, even with some small variations between them. Secondly, for all the scenarios, S_{11} values proved to be low and with not much interest to the problem when compared with the transmission coefficient results. With the S_{21} results it was possible to compute the attenuation results. The results in table 1 allow to take some conclusions: (1) The possible idea of a linear relation between the number of trees of the same characteristics and the attenuation proved to be wrong; (2) Looking at the results it is possible to say that by adding more trees, the attenuation increases. This can be specially seen when looking for the squared absolute value of the transmission coefficient. It can also be seen analyzing the attenuation rate, but it is important to refer that for the simulation of four trees side by side the dataset has larger dimensions which caused the value of the attenuation rate to be lower; (3) Finally, the statistic studies performed in all the scenarios showed that the higher attenuation values are not so abundant. However, this higher attenuation values did show a small increment in number with the adding of more trees.

VI. Designed Simulation Tool

RAFire consists on a function that defines an empirical approximation of the RF attenuation caused by the combustion of a tree specified with tree parameters at a given point in space and time. The tree parameters are inferred from FDS simulations. However, the developed numerical model will need to be updated and calibrated as knowledge is gained from further results from FDS simulations and measurement campaigns. The function will return zero attenuation if a point (x, y, z) does not fall inside the tree volume or if the time instant t falls outside the burning duration. Hence, the only output of the simulation tool is the RF attenuation. RAFire requires the following list of inputs by the user: (1) x_0, y_0 and z_0 define the location of the tree in the computational domain [m]; (2) t_0 defines the instant when the tree starts to burn [s]; (3) $TreeParameters$ is a vector that contains: Type of tree canopy, radius of tree canopy base (rcb [m]), height of tree canopy (hc [m]), height of tree trunk below canopy (hT [m]), duration of canopy burn ($tburn$ [s]) and maximum attenuation in linear units ($Att0$); (4) x,y and z define the point where attenuation is to be calculated [m];(5) t defines the instant where attenuation is calculated [s]; (6) vf defines the fire front velocity [m/s]; (7) phi defines the fire front propagation direction, defined by an angle [rad].

The attenuation computation needs to adapt to the different types of vegetation and also to the different possible ignition processes. Hence, the simulation tool distinguishes three different types of attenuation computation:

1) Low Vegetation: The first ignition method is dedicated to the shallow vegetation, typically grass and bushes. The fire propagation is typically more circular , propagating from the ignition point to all directions around it. The variable that sets the propagation of the fire versus time is $rfire$ and it is calculated with the following expression:

$$rfire = rcb \times \frac{t - tt0}{tburn} \tag{10}$$

where rcb is the radius of the tree canopy base, t is the instant where the attenuation is to be calculated, $tt0$ is the instant when the tree starts its combustion and finally $tburn$ is the duration that takes the whole tree to burn. This variable $rfire$ can be seen as a percentage of the tree radius that is consumed by the fire over time. As this fire spread is based on radius, it is important to compute the distance from the received (x, y, z) point to the initial point. Hence, this distance is calculated with the following expression:

$$r = \sqrt{(x - x0)^2 + (y - y0)^2}. \tag{11}$$

The third and final important variable in this approach is $zfire$ that sets the vertical spread of the fire with relation to the radial spread. This variable can be computed with the following equation:

$$zfire = hc \times \frac{|r - rfire|}{rcb} \tag{12}$$

where hc is the grass or bush height. After the computation of the above variables the RF attenuation can be finally calculated. In this fire propagation approach the attenuation is calculated if r is smaller than $\theta_{bush} \times rfire$. θ_{bush} is a parameter to be optimized through supervised or automatic learning from real data. At present, we arbitrate defined $\theta_{bush} = 1.2$. The attenuation suffered by an EM wave in one meter of propagation path, in linear units, can be computed with the following expression:

$$att_{shallow} = 1-(1-Att0)\times e^{-(\frac{r-rfire}{rcb})^2} \times e^{-(\frac{z-zfire}{0.4hc})^2} \tag{13}$$

2) Ignition process from below: The attenuation computation when the ignition process starts from below is based on relations between the height of the tree and also the radius of the tree canopy. Two new variables need to be

introduced: $zfire$ and rz. Even though $zfire$ also exists in the attenuation computation for shallow vegetation, they have different computation processes. The variable $zfire$ in this case stands for the height where the progressing fire is in that time t. The second one, rz, stands for the relation between the radius and height of the tree while the fire is progressing. The variable $zfire$ can be computed with the following expression:

$$zfire = hc \times \frac{t - tt0}{tburn} \tag{14}$$

where hc is the height of the tree canopy, t is the instant where the attenuation is to be calculated, $tt0$ is the instant when the tree starts burning and $tburn$ is the time that takes the fire to consume the whole tree. Hence, this variable is basically a percentage of the height of the tree canopy that evolves in time with the fire. On the other hand, the other new variable can be computed with the following equation:

$$rz = rcb \times \frac{hc - (z - hT)}{hc} \tag{15}$$

where rcb is the radius of the tree canopy base, hc is the height of the tree canopy and hT is the height of the tree trunk. After the computation of these two variables, the attenuation can be computed. As the variable rz sets the radius where the fire is, the attenuation is only computed if the received point is placed inside the circle with rz as a radius. In this case, The attenuation suffered by an EM wave in one meter of propagation path, in linear units, can be computed with the following expression:

$$att_{below} = 1 - (1 - Att0) \times e^{-\left(\frac{z - hT - zfire}{hc}\right)^2 / \left(10 \times (1 + \frac{zfire}{hc})\right)} \tag{16}$$

3) Fire Front: When compared with the above ignition processes, this one requires two more inputs that were mentioned in the previous section: the fire front velocity vf and the fire front direction defined by the angle ϕ. Consider a point P in the edge of the tree canopy base, with a tangent straight line L that passes from it. This point has the following coordinates:

$$P = (xp, yp) = (\rho \times cos(\phi) + x0, \rho \times sin(\phi) + y0) \tag{17}$$

where ρ in the beginning is equal to the tree canopy base radius. In addition, the center of the tree canopy as well as the radius (rcb), are given input parameters by the user. Using the point P and the position of the tree center and knowing that the line that connects them is perpendicular to the line L it is possible to compute its slope:

$$m_L = -\frac{1}{tan(\phi)} \tag{18}$$

After computing the slope and using again the coordinates of the point P it is possible to compute the line equation for the line L:

$$y + \frac{1}{tan(\phi)}x - y_p - \frac{1}{tan(\phi)}x_p = 0 \tag{19}$$

where (x_p, y_p) are coordinates of the point P that depend on ρ that describes the line of fire movement and given by:

$$\rho = rcb - vf \times (t - t0) \tag{20}$$

After defining ρ, one more variable it is necessary to describe the fire front movement in the tree canopy: $hfire$. This new variable defines the vertical progression of the fire in the tree canopy and it is dependent on ρ. $hfire$ can be computed with the following equation:

$$hfire = hT + (1 - \mid \frac{\rho}{rcb} \mid) \times hc \tag{21}$$

where hT is the height of the trunk and hc is the height of the tree canopy.

Hence, when receiving a point (x, y, z), if z is smaller than $hfire$ and if when replacing x and y in the equation 19 the result is smaller than the fire front depth θ_{front},

$$\mid y + \frac{1}{tan(\phi)}x - y_p - \frac{1}{tan(\phi)}x_p \mid \leq \theta_{front} \tag{22}$$

the attenuation suffered by an EM wave in one meter of propagation path, in linear units, can be computed with the following expression:

$$att_{front} = 1 - (1 - Att0) \times \ e^{-\theta \times (\frac{\rho}{\rho_0})^2} \tag{23}$$

where $Att0$ is a given input parameter and ρ_0 is equal to the tree canopy radius.θ_{front} and θ are parameters to be optimized through supervised or automatic learning from real data. At present, we arbitrate defined $\theta_{front} = 0.3$ and $\theta = 10$.

A. Total Attenuation

The presented att functions (13,16,23) compute the attenuation suffered by the EM wave in one meter of propagation path, in linear units, for a receiving (x, y, z) point that falls inside the tree volume. However, it is necessary to explain the computation of the total attenuation for one propagation path. Consider the same illustration of figure 5.4 but aiming to compute the total attenuation for $z = 2m$ and $z = 4m$. This problem illustration can be found in figure 10. As Att is the attenuation over one meter, the following relation can be computed:

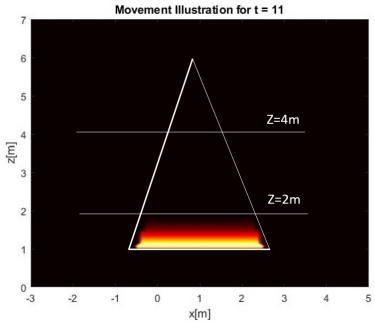

Fig. 10: Problem illustration.

$$att = e^{-\alpha x} \iff ln(att) = -\alpha \tag{24}$$

where $x = 1$m and α is the attenuation rate, in Np/m.

If we want to compute the attenuation for a length different than one meter, e.g. 16 cells Δx, the total attenuation in linear units can be computed with the following relation:

$$A = e^{\sum_{n=1}^{16} -\alpha \Delta x} = e^{\sum_{n=1}^{16} ln(att) \Delta x} \tag{25}$$

where n is the number of cells in the link and Δx it is the length of the cell.

Furthermore, if we want to compute the attenuation for a length different than one meter and crossing two trees, e.g. 16 and 7 cells Δx, the total attenuation in linear units can be computed with the following relation:

$$A = A_1 + A_2 = e^{\sum_{n=1}^{16} -\alpha_1 \Delta x} + e^{\sum_{n=1}^{7} -\alpha_2 \Delta x} \tag{26}$$

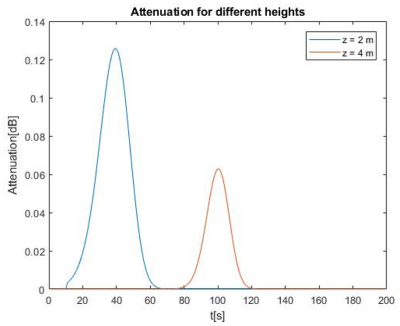

Fig. 11: Total attenuation for different heights.

Figure 11 shows the attenuation plot obtained with the described equations in this subsection for the presented example, where $\Delta x = 0.1$m. For the height $z = 2m$, the length of the link is larger. Hence, the attenuation presents a maximum value higher than for $z = 4m$.

VII. Experimental Work

During this work two types of measurement scenarios were envisioned: (1) Open environment scenarios where the transmitter and receiver are placed in front of each other with a linear or circular burner inserted in the middle of the propagation path; (2) Closed environment scenario, denominated the vortex generator scenario, where the combustion process takes place inside a chamber with whirling wind, in order to create a longer, higher and stable column of fire. This vortex chamber in a high squared cross-section structure, where two of the walls are made of glass, and the other two made of metal.

A proper setup was needed to acquire the reflection and transmission coefficients in these scenarios, both in frequency and time-domain. Hence, the experimental work during this work was divided into the following steps:

1) Design and fabrication of two ultrawideband antennas for fire inspection: For this work, two equal ultrawideband antennas were designed, to cover the 600-8000 MHz frequency range. The balanced antipodal Vivaldi antenna (BAVA) topology was selected for its known ultra wideband response. The antenna was designed using CST MWS, considering a low-cosr substrate (FR4). The final antennas, with dimensions 288x290 mm, were manufactured using printed circuit technology. Basic antenna tests were performed to confirm the design and performance in terms of its input reflection coefficient.

2) Measurement campaigns at the IT labs in Lisbon: Using alternative materials to represent fire, given that these labs do not have conditions to deal with real fire experiments, the objective was to test the measurement equipment and analysis algorithms in conditions closest as possible to the real scenario, to anticipate and solve possible issues to appear in real fire environment.

For the first tests of the antennas, a single antenna setup was used to measure the reflection from reference targets positioned a few meters away from the antenna. The chosen reference targets were a dihedral and a metal plane, due to its well-known scattering properties. Measurements were performed in the frequency range from 0.2 GHz to 14 GHz and all targets were placed at a distance of 1.99 m from the antenna. The targets were detected with success. These first measurements were especially important to determine the intrinsic delay introduced by the antenna.

Burning vegetation generates many gases and electrical particles that will contribute to the formation of plasma. Although it is not possible to use real fire in the Lisbon lab, representative tests still need to carried out to calibrate the system and algorithms before going to the real site, where only a one-shot burn will be possible. The plasma has a refractive index normally slightly bellow one. Therefore a well calibrated system, with proper dynamic range is required to detect its echo. This challenge was reproduced resorting to material with slightly higher than one refractive index: Styrofoam of different sizes, cardboard boxes with different dimensions, and cardboard boxes filled with polystyrene packing peanuts. In all cases the antenna and the algorithms were able to detected the targets with good accuracy. Furthermore, in most of the measurements we were able to compute the refractive index of the targets, based on the accurate detection of the time of arrival of the echo.

The vortex column is made of glass and metal. Therefore, the added challenge with the vortex scenario is that the RF probing signal passes through the glass wall twice, and further experiences reflection at the metal walls. The scattering from the fire column must be deembedded from this severely perturbed RF signal. In order to be able to confirm in advance the feasibility of the measurement, a replica of the vortex scenario was built: plexiglass was used to represent the glass wall, metal cabinets were used to represent the metal walls and styrofoam was used to represent the fire due to its refraction index close to one (even though that it is a static target). A metal target was also used to calibrate the position of the styrofoam.

An example for one acquisition, in transmission mode, is shown in figures 12 and 13. Figure 12 stands for the reference acquisition when the ”chamber” is empty whereas in figure 13 the styrofoam block is present as a target. The red lines show the distances where the different interfaces were expected. On the reference acquisition (figure 12), four important peaks are identified in the plot: (1) corresponds to the direct coupling between the two antennas; (2) corresponds to the reflection

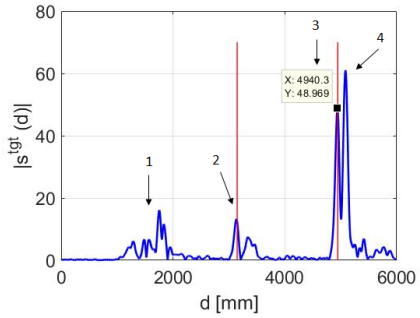

Fig. 12: Results for the replica of the vortex scenario when the cabin is empty. Reference measurement.

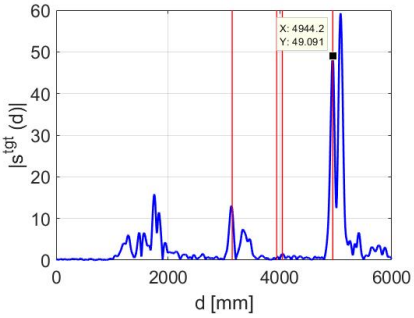

Fig. 13: Results for the replica of the vortex scenario when styrofoam is used as a target.

on the plexiglass slab; (3) corresponds to the reflection at the metal plane and it is the reference peak for transmission; (4) is the largest peak of all of them, and represents the corner formed by the cabinets. This corner behaves in a similar way as a dihedral, that is why its reflection is so intense.

Comparing the reference plot with the one with styrofoam we can highlight two important differences. Firstly, the red lines around 4000 mm set the position of the styrofoam block. Secondly, from the marked peak, it can be observed that it has a delay of 3.9 mm when compared with the reference, due to the styrofoam interposition. Using this delay, the distances and different angles in the setup, as well as the thickness of the styrofoam, one can compute the permittivity value for the styrofoam. In this case, the obtained value was 1.04 which is a plausible value for styrofoam. Overall these different measurements played a major role and showed that the setup was ready for the measurement campaign. Some important conclusions from the preparation phase were: (1) The direct coupling between antennas didn't impair the detection of the targets; (2) The different interfaces were detected at the expected distances; (3) The targets with low refractive indexes were detected in the right distances and it was possible to compute with accuracy its refractive index, proving that the setup was adequate to the different scenarios to be faced.

3) Measurement Campaign at Lousã: The first measurement campaign with actual fire was developed in Lousã, at the Laboratório de Estudos sobre Incêndios Florestais (LEIF), with the following objectives: (1) To understand the fire dynamics over combustion time; (2) To verify the fire front spread considering different scenarios; (3) To determine the relative permittivities of the fire flame, and possibly identify plasma characteristics. During the two days that composed this measurement campaign two following scenarios were faced: Linear and circular butane gas burner with and without additional pine needles load, vortex generator burning pine needles and bush vegetation and finally a canyon simulator filled with pine needles disposed in a "V" shape.

As an example of the obtained results and the performed post-analysis, data is presented for the vortex generator scenario. This relates to the preliminary measurement described in the previous subsection. The antennas were placed at the first level of the structure as it is possible to see in figure 14. The direct propagation path passes through the glass wall, through the fire and then reflects in the metal wall. This is the most challenging scenario faced in the measurement campaign due to the high refractive index of both the glass and metal and the low refractive index of the plasma.

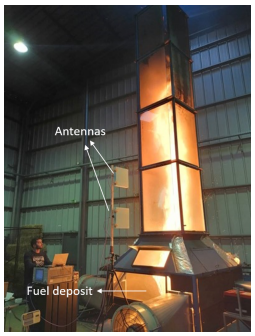

Fig. 14: Photos of the vortex generator on

The results for the vortex scenario with bush vegetation for one instant are shown in figures 15 and 16. The reference plot highlights that the lab mock-up used in Lisbon to prepare the measurement campaign was was a faithful representation of the real scenario. One can observe that, even though the intensity of the peaks are different due to the different refractive index of the involved materials, there are four different important peaks in the plot just like there were in figure 12. These peaks are highlighted with numbered arrows in figure 14 and represent: (1) Direct coupling between the two antennas; (2) Reflection on the glass; (3) The reflection in the metal plane, which is the reference peak for transmission between the antennas; (4) Reflection at the corner that is formed by the two metal walls in the vortex. Furthermore we can see in figure 16 that, when compared to the reference, the transmission peak with fire for that instant appears at a smaller distance, meaning the signal arrived faster, which is equivalent to saying that the medium had a refractive index lower than one as in a plasma.

Overall this first measurement campaign with real fire played a big contribution, with all the initial objectives being fulfilled. From the post-analysis, some important points can be highlighted: (1) The results in transmission mode produced more interesting results than in reflection mode; (2) The fire proved to have some influence on the link, specially when vegetation was used as an extra fuel; (3) Even though these were all very small scale fire experiments, in some of the acquisitions like the one showed in figure 16, the signal was

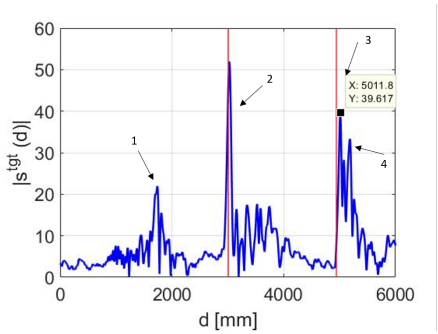

Fig. 15: Results for the vortex generator scenario empty. Reference measurement.

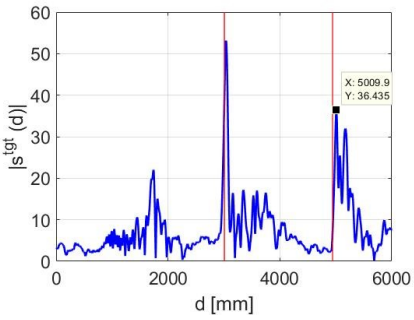

Fig. 16: Results for the vortex generator scenario burning bush vegetation.

received faster when compared with the reference, possibly indicating the presence of a medium with a refractive index lower than one like in a plasma; (4) This first measurement campaign was also especially important to identify the key experiments needed in the next measurement campaigns of the project and to parameterize the fire dynamics simulator.

VIII. Conclusions

Firstly, the experimental work performed during this thesis resulted in interesting results in transmission mode, showing that the fire did had some influence on the link. In the measurement campaign only small scale fire experiments were performed as the main goals were to calibrate the fire dynamics simulator and to see in a small scale how the link was affected by the flames. Hence, it is necessary for the project to do more measurement campaigns with larger volumes of vegetation. Secondly, the simulations showed maximum attenuation values between 3 and 7 dB depending on the number of trees. However, statistic studies showed that this maximum values are not continuous in time but happen mostly in just one voxel and in a certain instant. Therefore it is necessary to continue to use the measurement campaigns to calibrate the fire dynamics simulator. FDS is a very powerful tool but with long running times which cause some time constraints. However, it is important to run simulations for some other tree species with varying quantities and sizes. Lastly, RAFire computational performance gives good prospects for the future. Nonetheless, to reach its full purpose needs to be fed with larger numerical and experimental validation.

IX. Acknowledgements

The work was developed at Instituto de Telecomunicações, as part of the projects RESCuE-TOOL (PCIF/SSI/0194/2017) and UIDB/50008/2020, both funded by the Portuguese Government, Portuguese Foundation for Science and Technology (FCT).

References

[1] J. A. Boan, "Radio Propagation in Fire Environments," Ph.D. dissertation, University of Adelaide, Australia, 2009.
[2] H. F. Calcote, "Mechanisms for the formation of ions in flames," *Combustion and Flame*, 1957.
[3] M.L.Heron and K. M. Mphale, "Radio wave attenuation in bushfires, tropical cyclones and other severe athmospheric conditions," School of Mathematical and Psysical sciences, James Cook University, Australia, Tech. Rep., 2004.
[4] K. Mphale, "Radiowave Propagation Measurements and Prediction in Bushfires," Ph.D. dissertation, James Cook University, 2008.
[5] J. Boan, "Radio experiments with fire," *IEEE Antennas and Wireless Propagation Letters*, 2007.
[6] K. M. Mphale, P. V. Luhanga, and M. L. Heron, "Microwave attenuation in forest fuel flames," *Combustion and Flame*, 2008.
[7] D. Letsholathebe, K. M. Mphale, S. Chimidza, and M. L. Heron, "Radio Wave Propagation Experiment in Sugarcane Fire Environments," *Journal of Electromagnetic Analysis and Applications*, 2016.
[8] C. M. Dissanayake, M. N. Halgamuge, K. Ramamohanarao, B. Moran, and P. Farrell, "The signal propagation effects on IEEE 802.15.4 radio link in fire environment," in *Proceedings of the 2010 5th International Conference on Information and Automation for Sustainability, ICIAfS 2010*, 2010.
[9] É. Dieudonné, A. Kameni, L. Pichon, and D. Monchaux, "Radio frequency attenuation by rocket plume from ground study to in-flight prediction," *Applied Computational Electromagnetics Society Journal*, 2017.
[10] K. Kinefuchi, I. Funaki, and T. Abe, "Frequency-dependent FDTD simulation of the interaction of microwaves with rocket-plume," *IEEE Transactions on Antennas and Propagation*, 2010.
[11] K. Kinefuchi, K. Okita, I. Funaki, and T. Abe, "Prediction of in-flight radio frequency attenuation by a rocket plume by applying CFD/FDTD coupling," in *49th AIAA/ASME/SAE/ASEE Joint Propulsion Conference*, 2013.
[12] A. Pekmezci, E. Topuz, and L. Sevgi, "Finite difference time domain formulation for epsilon-negative medium using wave equation," *International Journal of RF and Microwave Computer-Aided Engineering*, 2016.
[13] S. D. Gedney, "Introduction to the Finite-Difference Time-Domain (FDTD)) method for electromagnetics," *Synthesis Lectures on Computational Electromagnetics*, 2011.
[14] W. Mell, A. Maranghides, R. McDermott, and S. L. Manzello, "Numerical simulation and experiments of burning douglas fir trees," *Combustion and Flame*, 2009.
[15] K. McGrattan, S. Hostikka, R. McDermott, J. Floyd, and M. Vanella, "Fire Dynamics Simulator User's Guide," *NIST Special Publication 1019 Sixth Edition*, 2019.
[16] A. Khurana, *Theory and Practice of Optics and Refraction*, ser. Modern system of ophthalmology. Elsevier India, 2013. [Online]. Available: https://books.google.pt/books?id=vp2BngEACAAJ
[17] K. Mphale and M. Heron, "Ray tracing radio waves in wildfire environments," *Progress in Electromagnetics Research*, 2007.
[18] L. Pedrotti, "Basic Physical Optics," in *Fundamentals of Photonics*, C. Roychoudhuri, Ed., 2008. [Online]. Available: https://doi.org/10.1117/3.784938
[19] K. Mphale and M. Heron, "Wildfire plume electrical conductivity," *Tellus, Series B: Chemical and Physical Meteorology*, 2007.
[20] ——, "Measurement of electrical conductivity for a biomass fire," *International Journal of Molecular Sciences*, 2008.
[21] ——, "Microwave measurement of electron density and collision frequency of a pine fire," *Journal of Physics D: Applied Physics*, 2007.
[22] D. Pozar, *Microwave Engineering Fourth Edition*, 2005.
[23] S. Faria, M. Vala, P. Coimbra, J. Felício, N. Leonor, C. Fernandes, C. Salema, and R. F. Caldeirinha, "Comparative Study of Computational Electromagnetics Applied to Radiowave Propagation in Wildfires," URSI GASS 2020.